# A General Framework for Subspace Detection in Unordered Multidimensional Data

## – Supplementary Material B –
## Standard Hough Transforms for Straight Line Detection as a Particular Case of the Proposed Subspace Detection Framework


Leandro A. F. Fernandes [a], Manuel M. Oliveira [b]

[a] *Instituto de Computação, Universidade Federal Fluminense (UFF)*
*CEP 24210-240 Niterói, RJ, Brazil*
*Tel +55 21 2629-5665, Fax +55 21 2629-5669*

[b] *Instituto de Informática, Universidade Federal do Rio Grande do Sul (UFRGS), CP 15064 CEP 91501-970, Porto Alegre, RS, Brazil*


## B.1 Description

This document presents a derivation of the standard Hough transform (HT) formulation for straight line detection in datasets comprised by points from the equations defining our subspace detection framework [1]. The derivations relating the parameter space of the standard HT for circle detection to the proposed parameter space is presented in Supplementary Material C. These results show that standard HTs are particular cases of our subspace detection scheme.


*Email addresses:* `laffernandes@ic.uff.br` (Leandro A. F. Fernandes), `oliveira@inf.ufrgs.br` (Manuel M. Oliveira).

*URLs:* `http://www.ic.uff.br/~laffernandes` (Leandro A. F. Fernandes), `http://www.inf.ufrgs.br/~oliveira` (Manuel M. Oliveira).

## B.2 The Standard Hough Transform

Duda and Hart [2] propose a HT that uses the normal equation of the line (B.1) while performing the line detection from points:

$$\rho = x\,\cos(\phi) + y\,\sin(\phi). \tag{B.1}$$

In (B.1), $(x, y)$ are the coordinates of points in the plane, $\rho \in [-R, +R]$ defines the distance from the line to the origin of the coordinate system of the 2-dimensional base space (*i.e.*, the center of the image plane), $\phi \in [0, \pi)$ is the angle between the $x$-axis and the normal to the line, and $R = \sqrt{w^2 + h^2}/2$ is the highest (positive) distance expected, for $w$ and $h$ being the width and height of the image, respectively.

The mapping procedure described by Duda and Hart defines $\phi$ as the arbitrated parameter, and $\rho$ as the parameter computed from a given $\phi$ value and from the $(x, y)$ coordinates of some input point.

## B.3 The Proposed Approach

Duda and Hart's formulation for the HT can be derived from our subspace detection framework by encoding input data points and intended straight lines into the homogeneous model of geometry (MOG). In such a MOG, the dimensionality of the representational vector space $\mathbb{R}^n$ is $n = 2 + 1 = 3$ (*i.e.*, the $d = 2$ dimensions of the base space plus the extra dimension imposed by the MOG), and the dimensionality of subspaces geometrically interpreted as straight lines is $p = 2$. As a result, the proposed model function for $p$-blades (*i.e.*, equation (15) in our paper [1]):

$$\mathbf{B}_{\langle p \rangle} = \boldsymbol{T}\,\mathbf{E}_{\langle p \rangle}\,\widetilde{\boldsymbol{T}}, \tag{B.2}$$

reduces to

$$\mathbf{B}_{\langle 2 \rangle} = \boldsymbol{R}_{3,1}\,\boldsymbol{R}_{3,2}\,\mathbf{E}_{\langle 2 \rangle}\,\widetilde{\boldsymbol{R}}_{3,2}\,\widetilde{\boldsymbol{R}}_{3,1} \tag{B.3}$$

by replacing the rotor $\boldsymbol{T}$ in (B.2) by its component rotor $\boldsymbol{S}_3$ and, in turn, replacing $\boldsymbol{S}_3$ by its component rotors $\boldsymbol{R}_{3,2}$ and $\boldsymbol{R}_{3,1}$ (see (23) and (18) in our paper [1]). Recall that

$$\mathbf{E}_{\langle 2 \rangle} = \mathbf{e}_3^* = -\mathbf{e}_1 \wedge \mathbf{e}_2 \tag{B.4}$$

in (B.3) is a canonical subspace used as reference (see (21) in the paper), and $\boldsymbol{R}_{3,2}$ and $\boldsymbol{R}_{3,1}$ encode rotations of $\theta^{3,2}$ and $\theta^{3,1}$ radians on the unit planes $\mathbf{e}_3 \wedge \mathbf{e}_2$ and $\mathbf{e}_2 \wedge \mathbf{e}_1$, respectively. The rotors $\boldsymbol{R}_{n,j}$ in (B.3) are defined as:

$$\boldsymbol{R}_{n,j} = \cos\left(\frac{\theta^{n,j}}{2}\right) - \sin\left(\frac{\theta^{n,j}}{2}\right)\,(\mathbf{e}_{j+1} \wedge \mathbf{e}_j)\,, \tag{B.5}$$

having $n = 3$ and $j \in \{2, 1\}$ in this example.

### *B.3.1 The Equivalence of Parameter Spaces*

The following derivations show how the rotation angles $(\theta^{3,2}, \theta^{3,1})$ characterizing 2-dimensional subspaces through (B.3) are related to the $(\rho, \phi)$ parameters in the normal equation of the line (B.1).

The basis vectors of the representational space $\mathbb{R}^3$ are $\{\mathbf{e}_1, \mathbf{e}_2, \mathbf{e}_3\}$. Under the homogeneous MOG, $\mathbf{e}_1$ and $\mathbf{e}_2$ are interpreted as directions parallel to the $x$ and $y$ axes of the image plane, respectively, and $\mathbf{e}_3$ (or $\mathbf{e}_0$ in the conventional notation of the homogeneous MOG – see Section A.3 in Supplementary Material A) is geometrically interpreted as the point at the origin. Notice that the reference subspace $\mathbf{E}_{\langle 2 \rangle}$ (B.4) is spanned only by the directional portion of the representational space (*i.e.,* vectors $\mathbf{e}_1$ and $\mathbf{e}_2$). As a result, $\mathbf{E}_{\langle 2 \rangle}$ is called an *improper line* (*i.e.,* a line at infinity [3]). However, as the rotor $\boldsymbol{R}_{3,2}$ is applied to $\mathbf{E}_{\langle 2 \rangle}$ ($\boldsymbol{R}_{3,2}\, \mathbf{E}_{\langle 2 \rangle}\, \widetilde{\boldsymbol{R}}_{3,2}$ in (B.3)), the vector factor $\mathbf{e}_2$ in $\mathbf{E}_{\langle 2 \rangle}$ rotates in the $\mathbf{e}_3 \wedge \mathbf{e}_2$ plane of the representational space and gets aligned to $\mathbf{e}_3$. Fig. B.1a shows that such an operation is geometrically interpreted as a translation along the line through the origin $\mathbf{e}_3$ with direction $-\mathbf{e}_2$. In practice, the improper line encoded by $\mathbf{E}_{\langle 2 \rangle}$ leaves the infinity and approaches the origin of the image plane as $\theta^{3,2}$ gets close to the $\pm\pi/2$ values. Thus, the parameter $\theta^{3,2}$ has a translation-like interpretation, as does have the $\rho$ parameter in the normal equation of the line (B.1). In fact, $\rho \equiv \tan(\theta^{3,2} + \pi/2)$.

The rotor $\boldsymbol{R}_{3,1}$ in (B.1) acts on the directional information of the line resulting from $\boldsymbol{R}_{3,2}\, \mathbf{E}_{\langle 2 \rangle}\, \widetilde{\boldsymbol{R}}_{3,2}$. Such a behavior can be derived from the rotation plane $(\mathbf{e}_2 \wedge \mathbf{e}_1)$ related to $\boldsymbol{R}_{3,1}$. Notice that a rotation in $\mathbf{e}_2 \wedge \mathbf{e}_1$ affects only the directional portion of the underlying representational space where data is being encoded. Fig. B.1b illustrates the subspaces (interpreted as straight lines) in Fig. B.1a after being transformed by a rotor $\boldsymbol{R}_{3,1}$ encoding a rotation of $\pi/3$ radians on the plane $\mathbf{e}_2 \wedge \mathbf{e}_1$. From these results, one can see that the $\theta^{3,1}$ parameter has the same interpretation of the $\phi$ parameter from the normal equation of the line (B.1), but in a different range of angular values. The former is defined in the $[-\pi/2, \pi/2)$ range, while the later is in the $[0, \pi)$ range. Such a difference may be compensated, leading to $\phi \equiv \theta^{3,1} + \pi/2$.

### *B.3.2 The Equivalence of Mapping Procedures*

In this example, we set the input entries for our approach as subspaces encoding points under the homogeneous MOG. We are restricting the type of input data in the following derivations because the HT proposed by Duda and

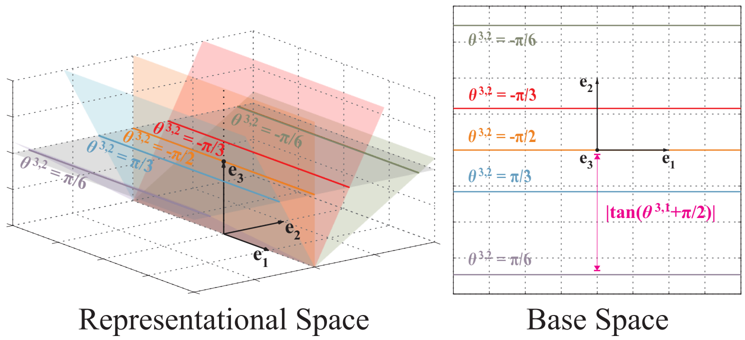


(a)

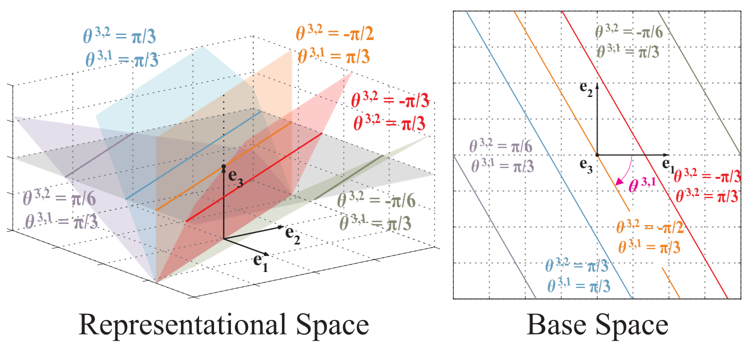


(b)

Fig. B.1. Geometric interpretation of the parameters defined by our approach when it is applied as a straight line detector on data encoded into the 2-dimensional homogeneous MOG. (a) The $\theta^{3,2}$ parameter encodes the distance of the lines to the origin of the base space ($\mathbf{e}_3$). Such a behavior can be seen in the top-right image, where straight lines are depicted in the base space. Such lines represent the geometric interpretation of the subspaces resulting from applying, on the reference blade $\mathbf{E}_{\langle 2 \rangle} = -\mathbf{e}_1 \wedge \mathbf{e}_2$ (B.4), rotations ranging from $-\pi/2$ to $\pi/3$ radians in the $\mathbf{e}_3 \wedge \mathbf{e}_2$ plane of the representational space (top left). (b) The $\theta^{3,1}$ parameter encodes the direction of the straight lines. It can be seen in the configuration obtained after applying a rotation of $\pi/3$ radians in the $\mathbf{e}_2 \wedge \mathbf{e}_1$ plane on blades depicted in (a).

Hart [2] expects points as input. In practice, however, the proposed mapping procedure is independent of the type of input entries.

In the homogeneous MOG, points are represented as vectors with the form:

$$\mathbf{x} = x\,\mathbf{e}_1 + y\,\mathbf{e}_2 + \mathbf{e}_3, \tag{B.6}$$

where $(x, y)$ are the coordinates of points, $\mathbf{e}_1$ and $\mathbf{e}_2$ are parallel to the image plane, and $\mathbf{e}_3$ is the basis vector related to the homogeneous coordinate.

The algorithm that maps input $r$-blades to $\mathbb{P}^m$ is presented in our paper [1] by Figs. 6 and 7, and it is described in Section 4.2.1 (the term "our paper" will be omitted from now on). The mapping algorithm is defined for input subspaces having dimensionality greater or equal to the dimensionality of intended subspaces. However, in the current example, the input subspace ($\mathbf{x}$ in (B.6)) is *one*-dimensional ($r = 1$), while the intended subspaces interpreted as straight lines are bidimensional ($p = 2$) in the assumed MOG. Thus, according to Section 4.2.1, one needs to take the dual of $\mathbf{x}$ as the used input ($\mathbf{X}_{\langle r \rangle}$ in Fig. 6), and to use the dual of $\mathbf{E}_{\langle 2 \rangle}$ (defined in (B.4)) as reference blade ($\mathbf{E}_{\langle p \rangle}$ in Figs. 6 and 7). By doing so:

$$\begin{aligned} \mathbf{X}_{\langle 3-1 \rangle} = \mathbf{x}^* &= (x\,\mathbf{e}_1 + y\,\mathbf{e}_2 + \mathbf{e}_3)^* \\ &= -x\,\mathbf{e}_2 \wedge \mathbf{e}_3 + y\,\mathbf{e}_1 \wedge \mathbf{e}_3 - \mathbf{e}_1 \wedge \mathbf{e}_2 \end{aligned} \tag{B.7}$$

and

$$\mathbf{E}_{\langle 3-2 \rangle} = \mathbf{E}^*_{\langle 2 \rangle} = (-\mathbf{e}_1 \wedge \mathbf{e}_2)^* = -\mathbf{e}_3, \tag{B.8}$$

reducing the mapping procedure to the case described in Section 4.2.1 (*i.e.,* $r \geq p$, because $r = 3 - 1 = 2$ in (B.7), and $p = 3 - 2 = 1$ in (B.8)). From the basis vector spanning the used reference blade $\mathbf{E}_{\langle 3-2 \rangle}$ (B.8), it follows that the set $\mathcal{E} = \{\mathbf{e}_3\}$. In this case, the spaces of possibilities $\mathbf{F}_l^{(t)}$ (used in Fig. 7) are:

$$\mathbf{F}_1^{(0)} = \mathbf{e}_3, \tag{B.9}$$

$$\mathbf{F}_1^{(1)} = \mathbf{e}_2 \wedge \mathbf{e}_3, \text{ and} \tag{B.10}$$

$$\mathbf{F}_1^{(2)} = \mathbf{e}_1 \wedge \mathbf{e}_2 \wedge \mathbf{e}_3. \tag{B.11}$$

In the first step of the mapping algorithm (Fig. 6, line 1), the set $\mathcal{P}^{(2)}$ is initialized:

$$\mathcal{P}^{(2)} = \left\{ (\mathbf{X}_{\langle 3-1 \rangle}, \varnothing) \right\},$$

where $\mathbf{X}_{\langle 3-1 \rangle}$ is given by (B.7). The (single) 2-tuple in $\mathcal{P}^{(2)}$ is processed during the first iteration of the loop (line 2 to 9, for $t = 2$), resulting in the set $\mathcal{P}^{(1)}$. In line 6, the *CalculateParameter* function is called in order to determine if the second coordinate of the resulting parameter vectors ($\theta^2$ in the algorithm, or $\theta^{3,1}$ in double-index notation) can be computed from $\mathbf{X}^{(2)}_{\langle 3-1 \rangle} = \mathbf{X}_{\langle 3-1 \rangle}$ or if it must be arbitrated. In this case, the parameter is arbitrated. Notice, by looking to (B.11) and (B.10), that there is no rotation on plane $\mathbf{P}^{(2)}_{\langle 2 \rangle} = \mathbf{e}_2 \wedge \mathbf{e}_1$ that, when applied to $\mathbf{X}_{\langle 3-1 \rangle}$, makes the transformed input subspace leave the tree of possibilities at $t = 1$. Actually, there is no 2-blade that can be spanned outside $\mathbf{F}_1^{(1)} = \mathbf{e}_2 \wedge \mathbf{e}_3$, because such a space of possibility does not include only one of the dimensions (*i.e.,* $\mathbf{e}_1$) of the total 3-dimensional space. Therefore, $\theta^2$ (or $\theta^{3,1}$) is arbitrated, as $\phi$ also is in the HT proposed by Duda and Hart [2].

By arbitrating the value of $\theta^2$ (or $\theta^{3,1}$), the set $\mathcal{T}$ in line 6 is initialized with values in the $[-\pi/2, \pi/2)$ range, chosen according to some discretization criteria (usually linear). In turn, $\mathcal{P}^{(1)}$ (line 7, Fig. 6) is updated by receiving 2-tuples comprised by blades computed as $\widetilde{\boldsymbol{R}}_2\,\mathbf{X}^{(2)}_{\langle 3-1 \rangle}\,\boldsymbol{R}_2$ and the possible (discrete) values of $\theta^2$. Recall that, according to the double-index notation, $\boldsymbol{R}_2$ corresponds to $\boldsymbol{R}_{3,1}$ (defined in (B.5)), as $\theta^2$ corresponds to $\theta^{3,1}$.

In the second iteration of the outer loop (Fig. 6, line 2 to 9), $t = 1$. Each element in $\mathcal{P}^{(1)}$ is processed during the inner loop (line 5 to 8), resulting in the set $\mathcal{P}^{(0)}$ with blades $\mathbf{X}^{(0)}_{\langle 3-1 \rangle}$ and the resulting parameter vectors. For all elements being processed, the current parameter ($\theta^1$, or $\theta^{3,2}$ in double-index notation) is computed by the *CalculateParameter* function. They are computed, rather than being arbitrated, because there is no guarantee that all possible rotations on plane $\mathbf{P}^{(1)}_{\langle 2 \rangle} = \mathbf{e}_3 \wedge \mathbf{e}_2$ make the transformed input subspace keep at least one vector factor inside the space of possibilities for $t = 0$ ($\mathbf{F}^{(0)}_1 = \mathbf{e}_3$ in (B.9)). For instance, $\mathcal{P}^{(1)}$ could include some blade

$$\mathbf{X}^{(1)}_{\langle 3-1 \rangle} = \mathbf{e}_1 \wedge \mathbf{e}_2,$$

which needs a rotation of $-\pi/2$ radians on plane $\mathbf{P}^{(1)}_{\langle 2 \rangle} = \mathbf{e}_3 \wedge \mathbf{e}_2$ in order to be transformed into

$$\mathbf{X}^{(0)}_{\langle 3-1 \rangle} = \widetilde{\boldsymbol{R}}_1 \, \mathbf{X}^{(1)}_{\langle 3-1 \rangle} \, \boldsymbol{R}_1 = -\mathbf{e}_1 \wedge \mathbf{e}_3,$$

*i.e.,* a subspace sharing at least one vector factor with $\mathbf{F}^{(0)}_1 = \mathbf{e}_3$. The only case that causes the value of $\theta^1$ (or $\theta^{3,2}$) to be arbitrated is when

$$\mathbf{X}^{(1)}_{\langle 3-1 \rangle} = \mathbf{e}_2 \wedge \mathbf{e}_3. \tag{B.12}$$

In such a case, the current blade already shares one vector factor with $\mathbf{F}^{(0)}_1$ and there is no rotation on plane $\mathbf{P}^{(1)}_{\langle 2 \rangle}$ that is capable to change $\mathbf{X}^{(1)}_{\langle 3-1 \rangle}$, because the subspace to be transformed (B.12) includes the rotation plane. However, the case depicted in (B.12) will never happen if one assumes subspaces written in the form (B.7) as input (*i.e.,* the dual representation of points under the homogeneous MOG). Notice that the expected input subspaces always have the $-1$ coefficient multiplying the $\mathbf{e}_1 \wedge \mathbf{e}_2$ basis blade in (B.7). Such a condition cannot be changed by arbitrating the previous parameter ($\theta^2$, or $\theta^{3,1}$), and hence, it will be kept while computing $\theta^1$ (or $\theta^{3,2}$). Thus, as in the HT proposed by Duda and Hart [2], the parameter $\theta^{3,2}$, related to $\rho$, is computed from the given input entry and a value arbitrated for $\theta^{3,1}$, or $\phi$.

The case depicted in (B.12) is likely to happen when the input subspace encodes the dual representation of directions, rather than points, under the homogeneous MOG. In such a case, the coefficient multiplying the basis vector $\mathbf{e}_3$ is *zero* in the direct representation of the direction, leading to a zero coefficient multiplying the $\mathbf{e}_1 \wedge \mathbf{e}_2$ basis blade in its dual representation. Notice, however, that directions are not accepted as input entries of the mapping procedure proposed by Duda and Hart [2]. Our approach, on the other hand, is independent of the type of input data.

It is important to emphasize that the *CalculateParameter* procedure (Fig. 7) is capable to identify that the values assumed by $\theta^2$ (or $\theta^{3,1}$) must be arbitrated, while the values assumed by $\theta^1$ (or $\theta^{3,2}$) must be computed in the current case study. However, in order to avoid the tedious evaluation of the procedure, such an identification was performed by using some geometric intuition about spaces of possibilities and the dimensionality of the given input blade rather than by running the algorithm in Fig. 7 of our paper [1], step-by-step.

## References


[1] L. A. F. Fernandes, M. M. Oliveira, A general framework for subspace detection in unordered multidimensional data, Pattern Recognit.(submitted).

[2] R. O. Duda, P. E. Hart, Use of the Hough transformation to detect lines and curves in pictures, Commun. ACM 15 (1) (1972) 11–15.

[3] L. Dorst, D. Fontijine, S. Mann, Geometric algebra for computer science: an object oriented approach to geometry, Morgan Kaufmann, 2007.